Sui et al. Geoenvironmental Disasters (2023) 10:15
https://doi.org/10.1186/s40677-023-00244-7

Geoenvironmental Disasters

RESEARCH

Experimental investigation on grout propagation in poured aggregates for controlling water inrush in tunnels with flowing water

Wanghua Sui[1*], Zongyuan Liu[1,2], Gailing Zhang[1], Deguang Mao[1,4], Ruijian Li[1,3] and Jinxi Liang[1,3]

Abstract

Background In recent years, the technology of blocking and grouting of has been widely used in the treatment of groundwater inrush in tunnels in China's mines. Studies have been carried out on the aggregates pouring under hydrodynamic conditions; however, there is lack of studies of the grout propagation in the pouring aggregate mass, which formed in the earlier stage. This paper presents an experimental investigation of grout propagation in poured aggregates with flowing water, which focused on the second stage, i.e., the grouting stage, after the first stage of aggregates pouring in the salvage of an inundated underground tunnel.

Results In this work, a visualized tunnel replica with flowing water was adopted to investigate the main effects of sealing efficiency, water pressure variation, propagation mechanism during grouting in the poured aggregates with different grain sizes and flowing water conditions. A series of experiments with orthogonal array design were carried out, and the propagation of cement/sodium silicate and the change characteristics of fluid pressure in the tunnel were obtained. The results show that the main effects on the sealing efficiency of grouting in poured aggregates with flowing water in a descending order is cement/sodium silicate ratio, relative density of aggregates, particle size distribution of aggregates, and final water pressure difference of both ends of aggregates segment. The cementation form of grouted aggregates has four types; T shape, H shape, O shape and shell shape. The main mode of grout propagation includes three types; permeation filling mode, compaction- permeation mode, and compaction-fracturing mode, which reflects the influence of grain size, density of aggregates and grouting pressure. The variation of water pressure can be divided into four categories; overall ascending type, step ascending type, concave type, and convex type. The curve type mainly depends on water pressure, water flowrate, relative density and grain size of aggregates, gel time, propagation mechanism of grout.

Conclusion The flow rate after grouting has decreased by approximately 60% to 86% compared to that before grouting, bulk hydraulic conductivity decreased by more than 80%, reflecting a great improvement of the sealing efficiency in the grouting stage after the pouring stage. The research on grout propagation in different graded aggregate mass has guiding significance for the design and construction of a rapid disaster treatment after groundwater inrush.

Keywords Groundwater inrush disaster, Inundated tunnel, Sealing efficiency, Grouting, Flowing water, Scale model, Cement/sodium silicate

*Correspondence:
Wanghua Sui
suiwanghua@cumt.edu.cn
Full list of author information is available at the end of the article

Introduction

Grouting and sealing projects for emergency relief in inundated mine tunnels are usually implemented in two stages: aggregate pouring and grouting (Hui et al. 2022). The aggregate pouring stage to construct a "water-blocking section" is a necessary prerequisite for the grouting stage, and at the same time, an effective grouting stage is the key to a successful water sealing (Fig. 1). The literature about the pouring stage was reviewed in the work of Hui et al (2022) and thus will not be repeated here for the sake of simplification. A visualized pipeline aggregate pouring experimental setup was developed (Jiang et al. 2020; Zhang et al. 2020; Hui et al. 2022), the influence of various factors on the effect of water plugging and aggregate settlement was analyzed, a criterion of water blockage of poured aggregate was proposed, drawing on sediment movement and slurry pipeline transportation theory. The results in the aggregate pouring stage constituted a base of this investigation.

The problems faced in the grouting stage should be investigated for a better understanding of its mechanism and a further appropriate design. The particularity in the

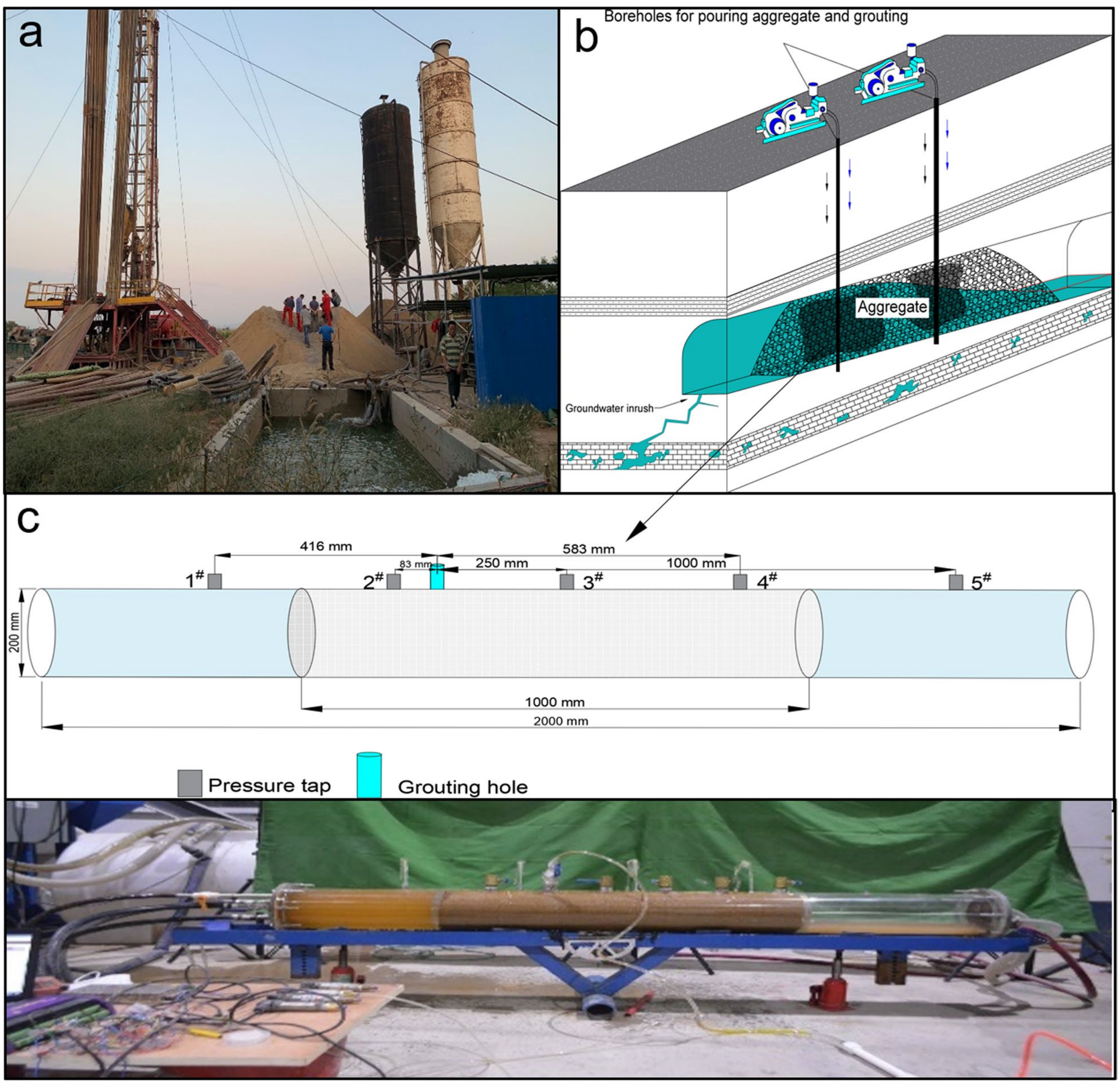

Fig. 1 Grouting in aggregates and its scale model **a** Site **b** Grouting stage **c** Tunnel replica scale model

grouting stage include that the grouting is carried out in a limited space, i.e., in a tunnel or roadway, with flowing water because there is still a water head difference at both ends of the poured aggregate mass, which has different densities because of unevenly pouring and water flushing.

Grouting in soil or rock mass with flowing water is often encountered in mine construction and production, especially in the rescue and disaster relief of groundwater inrush accidents, leakage prevention or anti-seepage grouting for flowing groundwater. The chemical grouting test under flowing water conditions shows two main effects of underground moving water on the chemical grouting of the soil: the grout penetration length to the grouting hole, and the shape of the grout propagation (Karol 2003). A propagation equation of the chemical grout in porous medium under flowing water conditions was theoretically deduced, compared it with the experimental data, resulting in that as the penetration radius of grout increases, the more serious the dilution of grout and difficult for solidifying (Ren 1982). An equation was then proposed to predict the movement of chemical grout front in flowing water (Gao and Sui 2016). Based on the investigation of the grouting of cement materials with different particle sizes under dynamic and static conditions, a theoretical prediction model of grout propagation was proposed (Mohammed et al. 2015). The diffusion mode of grout, empirical formula of grouting pressure and the grouting effect of multi-holes under hydrostatic conditions were studied, the characteristics of chemical grout gelling under flowing water conditions were analyzed, and the mechanical model of grout flow under dynamic water conditions was established (Wang 2011). Two-phase seepage theory was applied to describe the diffusion process of permeation grouting under dynamic water conditions, and the finite element model was used to analyze the propagation of grout under dynamic water conditions and the influencing factors of propagating range (Zhang et al. 2017). A comparative study of the propagation of chemically grouting in hydrostatic and moving water in a single fracture found that the diffusion of the grout in the static water is a gradually expanding circle centered on the grouting hole, while the diffusion of the grout in the flowing water is a changing oval. A mathematical formula for calculating the penetration length in a fracture considering the flow rate of water was then established (Zhan et al. 2011; Zhang et al. 2011).

The properties of grouting material are closely related to their performance and sealing efficiency. An optimal gel time of grout under given groundwater conditions, and the durability of chemical grouting in porous media were studied, a relationship curve between seepage speed and gelling time was established (Krizek and Perez 1985). The hydraulic conductivity of the coarse sand samples before and after chemically grouting showed that the chemical grouting obviously reduced the permeability of sand, and the hydraulic conductivity of chemical grout generally decreased with the increase of the confining pressure (Zhang 2016). The rheological characteristics of cement and phosphate sodium silicate were studied, and a suitable ratio of grouting materials and parameter for the actual project was selected (Ni 2014). A new cement impact grouting material (CIS) composed of Portland cement, coagulant sodium silicate and flocculant xanthan gum was developed, which has the advantages of short coagulation time, high early mechanical strength, high viscosity, high retention rate and non-toxicity (Li et al. 2019).

Sealing mechanism is one of the bases for determining grouting criterion and improving grouting design. Aiming at the problem of water inrush and fracture dynamic water grouting of rock mass, the propagation and sealing mechanism of grouting under dynamic water conditions of pipelines and fractures in rock mass was studied, and the corresponding grouting and sealing principles and conditions are respectively proposed (Hu 2016). Experiments on the control of sand and water flow in the inclined fracture model with chemical grout showed that the key to sealing the crack is to form a stable grouted sand layer. The viscosity of the slurry and the gelatinization trend of the slurry can not only reduce the water flow speed, but also increase the stability of sand grain deposition (Liang et al. 2019). The cross-sectional flow distribution, slurry movement and retention mechanism were studied numerically during the interception of the water-blocking sections (Mu and Dong 2020).

Grouting experiments are basically carried out in a limited space. A series of small-scale model compaction grouting tests performed in a geotechnical centrifuge and full-scale test in dry cohesionless soil showed that the grout bulb development is a function of the overburden pressure, injection rate, and grout composition (Nichols and Goodings 2000). A cavity expansion model of fracture propagation was proposed based on small-scale laboratory experiments of injection in particulate material (Chang 2004). Simulating the real environment of karst cavity, grouting tests such as in the filling clay under different initial compactness and grouting pressure were carried out, and mechanical and permeability tests were carried out on grouted reinforcement specimens (Liu et al. 2019). A large-scale grouting model with flowing water and simulation experiment of rapidly blocking dynamic water in tunnel were developed to study the propagation of cement and the rapid curing of grout (Li et al. 2016; Dong et al. 2020).

The above-mentioned research and engineering practice of grouting and water plugging can be as a reference for current study. The water plugging effect and migration of aggregates with different particle sizes under flowing water condition were considered in the existing model tests about aggregate pouring and grouting sealing in inundated tunnels. However, due to the hidden characteristics of grouting and plugging engineering, there is still a lack of investigation of grout propagation process and mechanism, pressure field, change of permeability, sealing effect and influencing factors in the grouting stage in the poured aggregate mass. Especially, the influencing factors of grouting and sealing effect and the retention and propagation in the aggregate mass need to be studied urgently, in the flowing water environment. Therefore, the purpose of this study is to conduct in-depth research on the grouting sealing effect and its influencing factors based on the previous research of the aggregate pouring stage, to provide a theoretical basis for the design and improvement for the grouting stage.

Materials and methods

Materials

Aggregates

According to the actual materials of grouting and aggregate pouring for water plugging project in coal mines (Table 1), four aggregate gradings with a particle size of 0.25–0.5 mm, 0.5–1 mm, 1–2 mm, and 2–10 mm, respectively, were selected in the scale model test.

Grouts

Two-liquid grout of cement slurry/sodium silicate was adopted in the test, which is used widely in mine water control engineering. P.O 42.5 ordinary Portland cement and sodium silicate with 42 Bé°were selected in the test. The preparation process is: first put the cement into the water, and use a beater to stir at high speed to make a cement slurry; the two slurries of cement and sodium silicate are mixed and injected into the aggregate mass in a tee tube by a two-liquid grouting device. After the two liquids meet, a chemical reaction occurs, producing a gelatinous substance.

Figure 2 shows 15 sets of gel experiments with different cement slurry/sodium silicate ratios under different water-to-solid ratios. It indicates that under the same

Table 1 Grading of aggregate used in grouting engineering

Name	Yellow sand	Centimeter-scale particle	Melon seed-sized particle	Slag-sized particle
Diameter (mm)	0.7–3	3–5	5–10	10–20

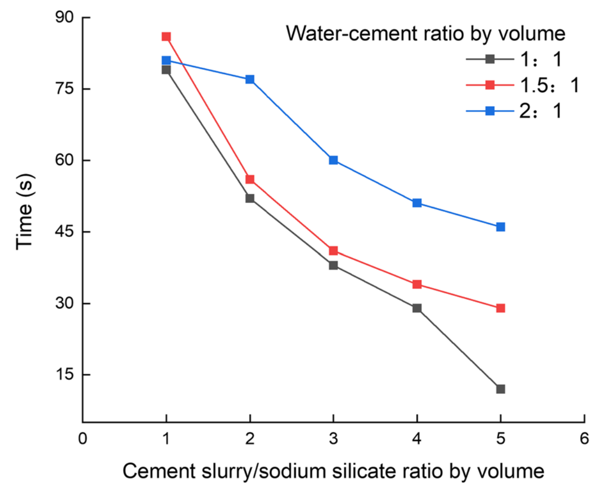

Fig. 2 Initial gel time of grouts with different cement slurry/sodium silicate ratios

conditions such as temperature, the initial gel time of the two-liquid slurry increases with the increase of the ratio of cement slurry/sodium silicate by volume, i.e., the more cement, the shorter the gel time. In the case of the same cement slurry/sodium silicate volume ratio, the greater the water-to-solid ratio, the longer the gel time. The gel time is significantly affected by the water-cement ratio, and in the case of other conditions unchanged, a relatively low water-cement within a certain range helps the gel time become shorter. In addition, temperature has an important influence on the gelling of two-liquid grout materials; this is the result of testing at an ambient temperature of 18 ℃, in a low temperature environment, the gelling time will become longer.

Tunnel replica

Tunnel replica is made of acrylic material poured with flanges at both ends of the pipe. The inner diameter of the circular pipe is 200 mm, the wall thickness of the pipe is 10 mm, the length of the pipe is 2000 mm, and there are 8 screw holes on the flange at both ends of the pipe. Screw hole with a diameter of 20 mm is connected to the high-pressure resistant flange plate through the sealing ring. There are 3 holes with a diameter of 35 mm in the flange plate. 5 pressure measuring holes with a diameter of 6 mm and 6 filling holes with a diameter of 25 mm were drilled at the upper side of the pipe. The flange plate is connected to the high-pressure pipe and drain pipe equipped with switches. The aggregate mass is fixed with an acrylic disc at each end. The disc is covered with holes of 8 mm in diameter to change the state of water flow and confine the aggregates. This study is mainly to study the grout propagation in aggregates, the friction coefficient of the boundary has little impact. The roughness of acrylic materials 1:20 can meet the requirements according to general hydraulic test.

Experimental setup

Grouting in the poured aggregate mass with different particle sizes in tunnel with flowing water is mainly affected by the force of gravity, viscosity and pressure that influence the water flow and the moving state of the grout. The flow in the experiments belongs to turbulent flow with a high flow rate, the force that plays a decisive role in the flow is gravity. When the hydraulic simulation is carried out, it is necessary to meet the Freud similarity criterion, Reynolds criterion, and Euler criterion to achieve dynamic similarity. However, it is difficult to meet the above all criteria at the same time. Therefore, if one of the Reynolds and Freud numbers of the two streams is ensured, the Euler number is equal, achieving a dynamic similarity. This experiment is based on the gravitational similarity criterion, because the main forces are gravity and seepage force. According to the gravity similarity criterion and the cross-sectional area of the coal mine tunnel, the similarity ratio is determined to be 1:20, considering the test model processing and test conditions. Figure 3 shows the experimental setup with a transparent tunnel replica to visualize the grouting process in different aggregates. The setup is mainly divided into four parts: variable head water supply, grouting, tunnel with flowing water and image data acquisition system. Five pressure measurement holes at the upper side of the tunnel replica are symbolized 1#, 2#, 3#, 4#, and 5# along the direction of water flow (Fig. 1c).

Fig. 3 Schematic of the experimental set up (①Water supply tank; ②Water storage tank; ③Data recording; ④Data acquisition; ⑤Grout storage tank; ⑥Tunnel replica; ⑦Air compressor; ⑧Water pressure sensor)

Experimental scheme and procedure

According to the case analysis of grouting treatment of water inrush in coal mine tunnel in recent years, an orthogonal test with four factors and four levels was carried out. The selected factors include particle size, final water pressure difference, cement slurry/sodium silicate ratio and relative density of aggregates, and each factor was selected at four levels.

Table 2 shows 16 trials of the designed orthogonal experiment $L_{16}(4^5)$. According to the gravity similarity criterion and the cross-sectional area of tunnel, considering the test model processing and test conditions, the geometric similarity ratio is determined to be 20. According to the gravity similarity criterion, the flow rate ratio was 4.47, and the design dynamic water pressure difference was 15, 20, 25 and 30 kPa, respectively. Different head differences were achieved by means of variable head devices. Water-cement ratio was selected to be 1.5:1, cement slurry/sodium silicate ratio was set in four levels: 1:1, 2:1, 3:1 and 4:1.

Results and analysis

Sealing efficiency

Sealing efficiency (*SE*) is calculated by collecting the water flowrate in the outlet of tunnel replica during the test:

$$SE(\%) = (Q_0 - Q_t)/Q_0 \times 100\% \tag{1}$$

where Q_0 and Q_t are flowrate of pre-grouting and post-grouting, respectively. Sealing efficiency can be divided into six grades: $90\% \le SE$, excellent; $80\% \le SE < 90\%$, good; $50\% \le SE < 80\%$, fair; $30\% \le SE < 50\%$, poor;$10\% \le SE < 30\%$, very poor; $SE < 10\%$, fail (Sui et al. 2015).

The results of the orthogonal experiment with 16 arrays indicated that the sealing efficiency ranges from 56.3 to 86% under a room temperature of 18 °C. Among them, the sealing efficiency for Trial nos.4, 7 and 10 is the grade good; while other 13 trials belong to the grade fair.

Main effects

The result of range analysis indicated that the sealing efficiency is influenced by the four factors, when single factor being considered, in the following descending order: cement slurry/sodium silicate ratio *C*, relative density of aggregates *D*, particle size of aggregates *A*, and final water pressure difference *B* (Table 3 and Fig. 4). According to the influence of the factors and levels calculated by the 16 trials on the average sealing efficiency, the optimal factor and level can be selected, i.e., $A_2B_2C_4D_4$. The sealing efficiency of Trial no.4 in the orthogonal test is the highest, i.e. $A_1B_4C_4D_4$, with a

Table 2 Orthogonal array design of L_{16} (4^5) for grouting in aggregates masses in a tunnel replica with flowing water

Trial no.	Symbol	Factors and levels				SE (%)	Grade
		Particle size A (mm)	Final water pressure difference B (kPa)	Cement slurry/sodium silicate ratio C	Relative density of aggregates D		
1	$A_1B_1C_1D_1$	0.25–0.5	15	1:1	0.25	56.9	Fair
2	$A_1B_2C_2D_2$	0.25–0.5	20	1:2	0.5	61.7	Fair
3	$A_1B_3C_3D_3$	0.25–0.5	25	1:3	0.7	75.8	Fair
4	$A_1B_4C_4D_4$	0.25–0.5	30	1:4	0.9	86.0	Good
5	$A_2B_1C_2D_3$	0.5–1	15	1:2	0.7	76.2	Fair
6	$A_2B_2C_1D_4$	0.5–1	20	1:1	0.9	74.3	Fair
7	$A_2B_3C_4D_1$	0.5–1	25	1:4	0.25	81.0	Good
8	$A_2B_4C_3D_2$	0.5–1	30	1:3	0.5	69.0	Fair
9	$A_3B_1C_3D_4$	1–2	15	1:3	0.9	79.8	Fair
10	$A_3B_2C_4D_3$	1–2	20	1:4	0.7	82.9	Good
11	$A_3B_3C_1D_2$	1–2	25	1:1	0.5	62.7	Fair
12	$A_3B_4C_2D_1$	1–2	30	1:2	0.25	65.6	Fair
13	$A_4B_1C_4D_2$	2–10	15	1:4	0.5	75.2	Fair
14	$A_4B_2C_3D_1$	2–10	20	1:3	0.25	69.3	Fair
15	$A_4B_3C_2D_4$	2–10	25	1:2	0.9	66.3	Fair
16	$A_4B_4C_1D_3$	2–10	30	1:1	0.7	56.3	Fair

Table 3 Range analysis for main effects on *SE*

For levels	Particle size A	Final water pressure difference B	Cement slurry/sodium silicate ratio C	Relative density of aggregates D
SE_1	70.1	72.02	62.55	68.2
SE_2	75.13	72.05	67.45	67.15
SE_3	72.75	71.45	73.48	72.8
SE_4	66.78	69.22	81.28	76.6
Range	8.35	2.83	18.73	9.45

sealing efficiency of 86%, which coincides basically with the optimal combination of factor and level.

The results of the analysis of variance also show that the cement slurry/sodium silicate ratio is most significantly affected by $F_C > 9.28$ with $\alpha = 0.05$ and a confidence level of 0.95 (Table 4).

The cement slurry/sodium silicate ratio C has more effect on the sealing efficiency than particle size of aggregates A, and final water pressure difference B and relative density of aggregates D. In the actual project of grouting, the final water pressure difference cannot be artificially intervened, and the formation of aggregates gradation and relative density is mainly determined in the pouring stage, therefore, the sealing efficiency can be controlled mainly by adjusting the grout mix in the grouting stage.

Pore water pressure during grouting

Figure 5 shows the variation of pore water pressure at different measured points of some examples among total 16 trials during grouting. The curves can be divided into four categories combined with phenomenon in tests; an overall ascending type, step ascending type, concave type, and convex type.

Overall ascending type

Figure 5a shows an example of water pressure changes of the overall ascending type in Trial no. 1. The measurement in sensor no. 4 was not discussed due to its incorrect monitoring data. Water pressure in the tunnel replica is basically stable before grouting from 0 to 80 s. Grouting which begins at 80 s results in water pressure gradually increase with multipeak fluctuations. Every

Table 4 Variance analysis for main effects on *SE*

Source of deviation	Deviation sum of squares	Degree of freedom	Mean square error	F ratio	*P* value	F0.05 (3.3) critical value
Particle size *A* (mm)	154.39	3	51.46	2.42	0.244	9.28
Final water pressure difference *B* (kPa)	21.46	3	7.15	0.34	0.803	9.28
Cement slurry/sodium silicate ratio *C*	782.26	3	260.75	12.24	0.034	9.28
Relative density of aggregates *D*	228.49	3	76.16	3.58	0.162	9.28
Error	63.91	3	21.30			

fluctuation with an increase and a decrease reflects a process of plugging and breaking of pathway. Fluctuation of water pressure lasts about 200 s. At about 400 s, water pressure in sensor no.5 in downstream water flow decreases gradually, this is because the gel time is short for the grout with a cement slurry/sodium silicate ratio of 1:1. This implies a gradual gelation of grouts in tunnel replica and a formation of a water-blocking section. A small final water pressure difference of 15 kPa also produces water pressures in sensors no.1, 2 and 3 increase and that in sensor no.5 decrease till grouting stop. It was observed that during grouting the grout propagated in aggregates to form a grouted mass first, then move upwards along the interface between grouting hole and aggregates, and downstream along water flow.

Step ascending type

Figure 5b shows an example of water pressure change of the step ascending type in Trial no. 16. When grouting begins at 180 s, a relatively large change of water pressure was observed with a preliminary sealing of grouting. The main reason is possibly a relatively large final water pressure difference between the both ends of the aggregate section, which is 30 kPa in Trial no. 16. With the gelation of grouts, gelled mixed mass accumulates gradually to form a larger effect of water blocking and cause another jump of water pressure. Trial no. 7 also presents a step ascending type of water pressure, with a final water pressure difference between the both ends of 25 kPa. The size of voids among aggregates in Trial no. 16 is larger than that in Trial no. 7; therefore, every jump of pressure for Trial no. 16 needs longer time. This implies more difficult retention of grouts in coarser aggregates.

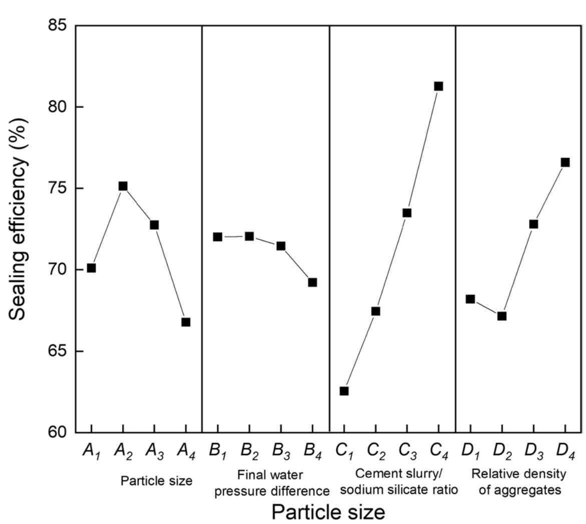

Fig. 4 Response graph for the main factors according to Table 2

Concave type

Figure 5c shows an example of water pressure change of the concave type in Trial no. 4. The water pressure gradually increased to 32.5 kPa after grouting beginning. The increase of water pressure is mainly because the small grain size of aggregates and small voids among them, and fracturing around grouting hole making pressure increase in the tunnel replica. The peak of water pressure reaches nearly 45 kPa at time 290 s. After this moment, the grout with semi-condensed state was broken by water flow, which results in a cliff-like decline during 300 s and 370 s. The similar decline occurred during 600 s and 700 s. During the period, after 550 s, the grouts gradually concentrated at the pathway that was broken in the previous period, and the pressure gradually recovered. It also makes the pressure required for the formation of a secondary breakthrough from 600 to 700 s greater than that required for the first-time breakthrough.

Convex type

Figure 5d shows an example of water pressure change of the concave type in Trial no. 9. The water pressure exhibits an overall increase trend during grouting. Grouts move to aggregates accumulation after the beginning of grouting at 80 s. The water pressure increases from 120 s and shows a convex type overall. Off course, there are several circles of increase and decline during the whole process. The grain size in this trial is relatively large and water flowrate relatively small. The initial gel time for the grouts is 41 s, which means a shorter time for the grout from the state of fluid transmitted to solid state, resulting in

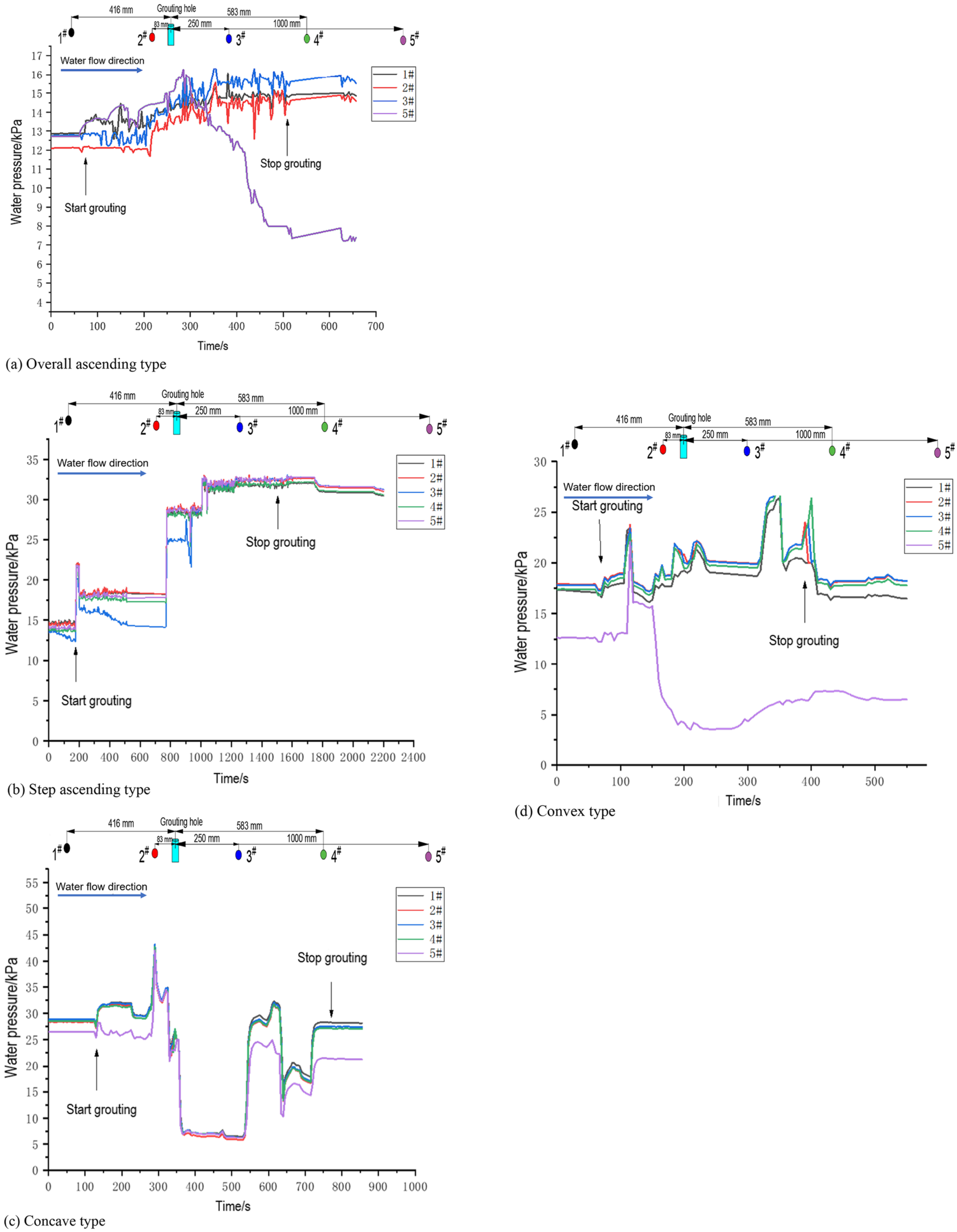

Fig. 5 Water pressure variation during grouting **a** an example of overall ascending type (Trial no. 1) **b** step ascending type (Trial no. 16) **c** concave type (Trial no. 4) **d** convex type (Trial no. 9)

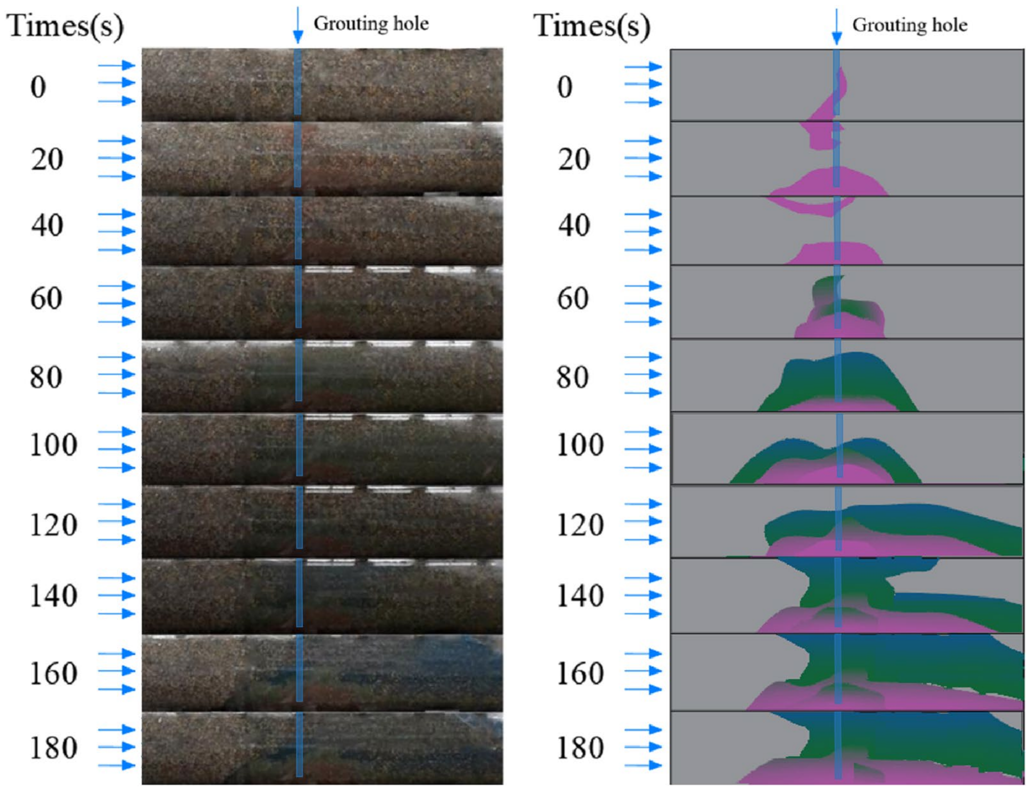

Fig. 6 Grout propagation in poured aggregates in Trial no. 13 **a** photo **b** image

easier gelation of grout. At 150 s, most of the water flow have been blocked, and the pressure in sensor no.5 has dropped obviously. Propagation range become larger with continuing grouting till stopping at 400 s. Afterwards, water pressure remains stable and shows a good sealing efficiency.

Grout propagation process

Figure 6 shows the propagation process for Trial no. 13. In order to observe the process of the grout over time, the grout propagation was revealed through different colors. The injection order is red, green, and blue. The grouting outlet is in the lower part of the acrylic pipe, 10 mm from the lowest point of the bottom. The grout enters the tunnel replica at an initial speed and begins to propagate under grouting pressure, gravity, and the dragging force of the water current. The direction of the water flow is from the left to the right, the grout mainly spreads along the direction of water flow. After grouting stops, the final pattern appears as: (1) The red grouts spread in a shape of a dune. The angle of upstream propagated slope is larger than that of downstream. This is because a sudden change of water flow rate occurred, i.e., decreased at downstream and increased upstream. (2) The green grouts spread continuously and extended to the middle and downstream end of the tunnel replica. The shape is similar to that of red grouts. The angle of propagated slope becomes small compared to that of red grouts. (3) The blue grouts distributed like a hillside with a relatively steep angle at upstream and a gentle slope downstream. The grouts have reached to the top. The rear extends to the end of the poured aggregates. Due to the formation of grouted mass by the early red and green grouts, the water flow speed in the back-water side is reduced, which is conducive to the deposition and propagation of grouts.

Grout propagation shape

After the grouting of every trail was completed, the grout and aggregate formed a consolidated mass. Then, the tunnel replica was cut from different directions to observe the shape of grouted mass. The shape of grouted mass can be divided into four types from the view of cross-sectional direction; an O shape, T shape, H shape and shell shape.

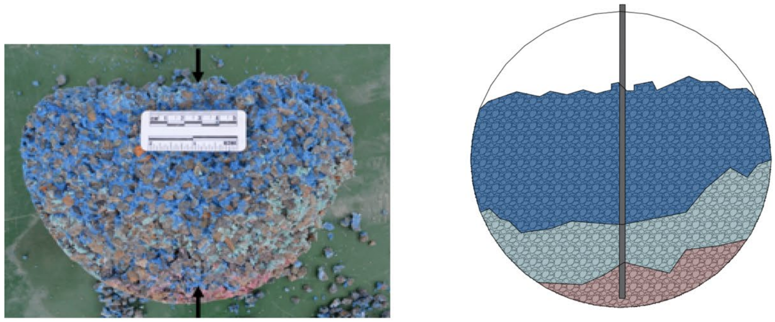

(a) Trial no. 13

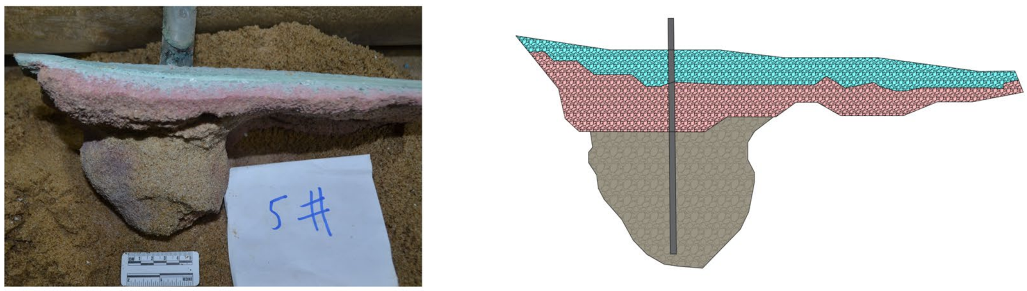

(b) Trial no. 5

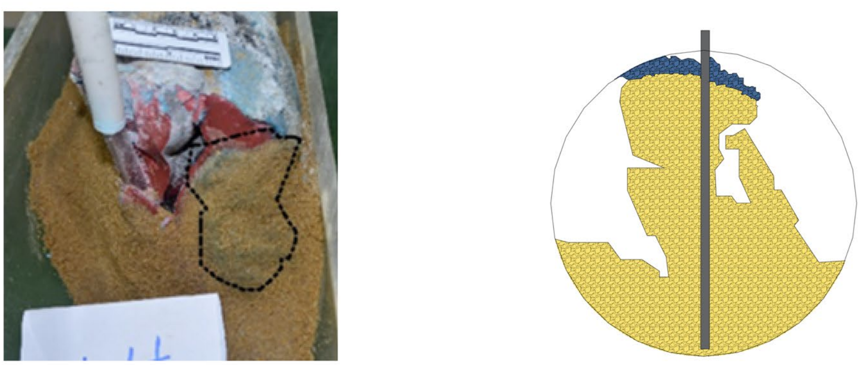

(c) Trial no.1

(d) Trial no. 11

Fig. 7 Cross-sectional shape of grout propagation in poured aggregates with flowing water **a** Trial no. 13 **b** Trial no. 5 **c** Trial no.1 **d** Trial no. 11

O shape

Grouts mainly spread by permeation layer by layer from the bottom to the top, and finally form a partially circular shape propagation cross section. It is a common propagation shape of grouts in coarse aggregates. Figure 7a shows the cross-sectional propagation of Trial no. 13, whose propagation along length direction is shown in Fig. 6. The three colors of red, green, and blue presents the position of grout propagation at different times. The grouted mass has a cylindrical shape with a length of 900 mm and a radius of 100 mm. There are with more voids at the top, not filled with grouts. The layered propagation phenomenon was described above, which happened in the previous stage of grouting in the flowing water. That is, the cement slurry/sodium silicate grout first forms a deposition layer at the bottom of the aggregates, and the red, green, and blue grout deposits layer by layer in the aggregate mass.

Due to large void in the aggregate mass and fast water flow, after the grouts enter the aggregates, the attachment of large particle aggregates makes a part of grout deposit at the bottom of the aggregates, and the rest diffuses downstream with flowing water. The grout diffusion in large particle size aggregates is better, and the sealing efficiency is high. As the grouts gelled, the grouts gradually block the area except for the top part of the tunnel replica. However, because the water flow rate in the top channel gradually increases with the sealing of lower part, the retention of grout becomes difficult, making it often difficult to block the top area for the O shape propagation.

T shape

Grouts firstly form a nearly round compaction grouted mass in the bottom, then spread into the upper part even to the top of tunnel replica, finally form a T shape like propagation cross section. It is a common propagation shape of grouts in medium and coarse aggregates. Figure 9b shows a cross-sectional propagation of Trial no. 5, and the grouts with different colors were added at different times and injected into the aggregates mass.

The grouted mass of Trial no. 5 consists of two parts. The first part is a plate-like consolidated mass at the top, approximately 250 mm long and 120 mm wide. The second part is a spherical shape with a diameter of approximately 100 mm. The surface of the grouted mass is rough and there is adhesion of sand particles. After cutting the grouted mass layer by layer in the direction perpendicular to grouting hole tube, the internal cementation of the spherical grouted mass was found to be intact. The cementation in the core is the best, forming slurry bubble of double liquid, with a higher strength and gelling effect injected at different time periods. The farther away from the core of the spherical solid, the worse the cementation, and easier the sand particles fall. The results show that the formation of the grouted mass can be divided into two phases. The first one is a round propagation and cementation in aggregates stage. In this stage, the grouts diffused in all directions evenly from the center of the outlet under grouting pressure. The compaction mainly occurred to form a nearly spherical diffusion inside the aggregate particles, of which part of the grouts penetrates inside the aggregates to form a grouted mass. The second stage is the propagation of grouts in the top of the tunnel replica. With grouting continues, the permeation around the outlet reaches its limit, and it is hard to penetrate the lower aggregate segment. The excess grouts are strumming up along the grouting tube to reach loosely accumulated areas at the top of the tunnel replica. Part of the grouts diffuse into the aggregates at the top and begins to solidify rapidly. The aggregate at the top is looser than that at the bottom, the aggregate void is larger, and the grout is easily enriched. While being carried by the water flow to the top and deposited, the rest of the grout flows downstream under the action of flowing water, and gradually flocculated during the process. Some of the flocculated grout is deposited on both sides of the void at the top of the tunnel replica and then gradually develops towards the top of the aggregate until topped.

H shape

Grouts mainly spread around grouting hole forming a column propagation, then penetrates the bottom and top of the tunnel replica, and finally form an H shape like grouted mass. It is a common propagation shape of grouts in fine aggregates. Figure 7c shows the cross-sectional propagation of Trial no. 1. The grouted mass of Trial no.1 consists of two parts. The first part is a cylindrical column consolidated mass with a diameter of 100 mm around grouting tube and the grouted mass at the top of the tunnel replica. The surface is relatively rough. The second part is the grouted aggregate at the bottom of the tunnel replica, 200 mm long and 60 mm high, and there is a columnar grouted body formed by fracturing along the dominant surface, showing a fingering to penetrate the aggregate.

The first part of the grouted mass is cut by taking the grouting tube as the axis of symmetry, the grouts are evenly distributed in a layer with a mixing sand layer, a smooth and flat surface, which indicates a good grouting fracture. The second part of the grouted mass is consolidated along the direction of water flow, the grouts mainly include the excess sodium silicate that has not reacted with the cement, and the aggregates are cemented at the bottom with a state of brittle and loose.

The results show that grouts penetrate aggregates around the grouting tube first and form a cylindrical grouted mass. At the same time grouts penetrate the bottom aggregates under gravity and flowing water to form a bottom grouted mass. After the formation of columnar grouted mass, grout hardly penetrates aggregates and reached to the top of the tunnel replica in reverse and flowed and finally enriched in the top and form a top grouted mass and gelled grouts.

Shell shape

Grouts mainly penetrates and fills the aggregates near the top of tunnel replica, while there is no grout penetrating in the lower part of aggregates. Grouts spread only in the surface i.e., spread along the dominant pathway on the top to form a shell shape. It is a common propagation shape of grouts in fine aggregates, or some special cases, such as large water pressure difference, short gel time, induce that the grouts have not yet gelled before being washing downstream. Figure 7d shows a cross-sectional propagation of Trial no. 11. The main reason is the small void between aggregates makes propagation difficult in them. Therefore, the grout propagates along an easier pathway on the top.

Grouting mechanism

Grouts penetrate the accumulated aggregates mass under grouting pressure. The factors such as size of void among aggregate particles, grouting pressure, gel time, water flow speed, hydraulic gradient will cause different propagation patterns due to different grouting mechanisms. The investigation of grouting mechanism and propagation pattern in aggregates is helpful to reveal the grout transportation and propagation when grouting in flowing water with concealment. The scale model experimental results indicated three diffusion mechanisms and modes, including permeation and filling, compaction-permeation, and compaction-fracturing.

Permeation and filling

After the aggregate was poured, the pipeline flow in the tunnel becomes a seepage flow, except for the larger flow rate in the residual top section, while water flow is slower in the rest part. The voids formed by the coarse aggregates are connected to each other to form a seepage pathway, and the grouts enter the saturated aggregates and propagate, which is a process of "grouts replacing water". After the grouts enter the coarse voids, they gradually penetrate the aggregates voids under the action of moving water. The force on the grouts includes gravity vertically and the drag force horizontally. The grouts gradually propagate in both directions along water flow and vertically. Figure 8a shows that the cement slurry/sodium silicate stained with red water-based dyes is injected into the aggregates during 0 to 360 s, forming a comet trail-like sedimentary flow zone in the tunnel replica (see also in Fig. 6). The green grouts injected from 360 to 860 s develops in the longitudinal and downstream directions, and the grouts infiltrated, filled, and accumulated. Finally, the blue grouts are injected and the diffusion continues to penetrate and block the residual pathway of the upper cross-section.

Compaction-permeation

The aggregate particle size is small, relatively dense, less permeable, and it is difficult for the grouts to penetrate the aggregates for a short period after entering the poured aggregates. Under the action of grouting pressure, the grouts squeeze the surrounding aggregates, and the particles near the outlet of grouts are compacted to form a grouted mass with a certain scale, and a mainly spherical or cylindrical shape. After the radii R reaches its limit, the grouts begin to partially permeate into the nearby aggregate voids, cementing the aggregate particles. Figure 8b shows that the Zone I is a compaction zone in the Trial no. 5. After the maximum penetration length R is reached, the cement slurry/sodium silicate begins to penetrate the surrounding particles to form the Zone II, a permeation zone.

Compaction-fracturing

After grouts gathered near the grouting hole and compressed the surrounding aggregates in the beginning period of grouting to form Zone I, when the pressure reached the fracturing pressure, part of the grouts split along the weak discontinuities in the surrounding aggregates. And this propagation mode mainly occurred in the loose aggregates accumulated in the upper part of the tunnel replica. Figure 8c shows that the blue colored grouts spread upward along the gap between the grouting tube and the aggregates to reach the aggregates accumulated in the upper part of the tunnel replica to fracture the red aggregates in the Trial no. 1. In the compaction-fracturing propagation mode, the cleavage vein mainly plays a role of squeezing the surrounding particles and skeleton, which improves the strength and impermeability of the aggregate accumulation.

Permeability variation pre- and post-grouting

Pouring aggregates transform the state of water flow in the tunnel from a pipe flow to a permeated flow, which basically and obeys the Darcy's law due to the flow speed was reduced greatly. The bulk hydraulic conductivity of the accumulated mass for pre-grouting and post-grouting can be determined according to the flow rate and

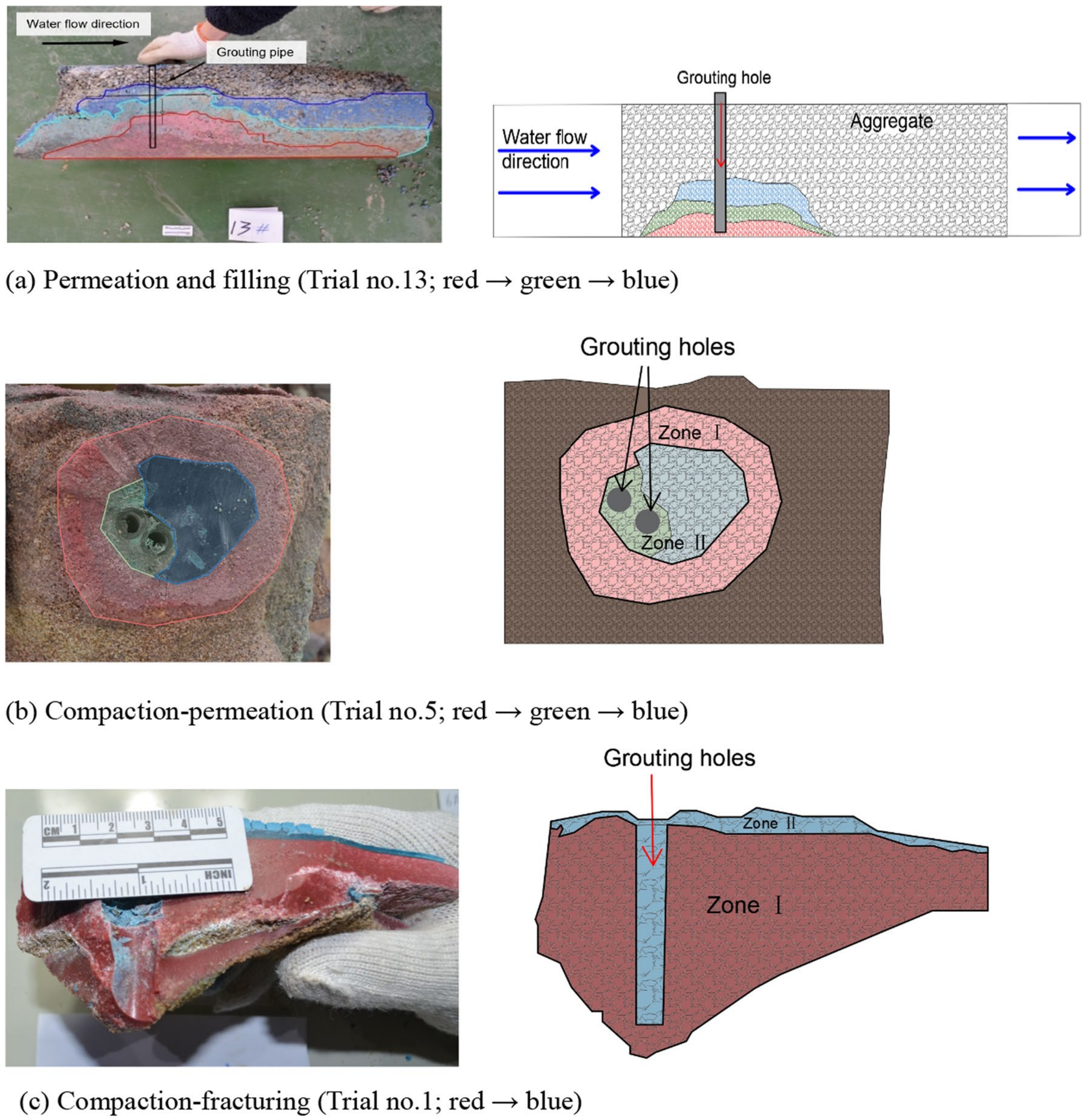

Fig. 8 Grouting mechanisms in aggregates **a.** permeation and filling (Trial no. 13; red → green → blue) **b.** compaction-permeation (Trial no. 5; red → green → blue) **c.** compaction-fracturing (Trial no. 1; red → blue)

hydraulic gradient along the deposited aggregate segment. Table 5 lists the hydraulic conductivity of the 16 trials pre- and post-grouting. If a reduction rate of permeability *RR* after grouting is defined as the ratio of the reduction of hydraulic conductivity of pre-grouting k_{pre} against that of post-grouting k_{post}, that is

$$RR(\%) = \left(k_{\mathrm{pre}} - k_{\mathrm{post}}\right)/k_{\mathrm{pre}} \times 100\% \tag{2}$$

The result of *RR* for each trial is the same to those of *SE* if Darcy's law is assumed to be obeyed. However, this hydraulic conductivity does not reflect the real hydraulic conductivity of grouted aggregates, because there are some cross-sections are sealed off while still some cross-sections not be sealed off. It is just a represented or an equivalent presentation of permeability of the entire grouted segment. Of course, the water flow mainly comes from the unsealed section part.

Discussion

Theoretical analysis of grouting propagation

Point grouting from the top of tunnel

If a point grouting from the top of the tunnel is conducted, the propagation of grout in the pored aggregates can be considered as a combination of the vertical and

Table 5 Hydraulic conductivity of pre- and post-grouting

Trial no.	Hydraulic conductivity (cm/s)		Reduction rate (%)
	Pre-grouting	Post-grouting	
1	0.63	0.27	56.9
2	0.32	0.12	61.7
3	0.25	0.06	75.8
4	0.34	0.05	86.0
5	0.59	0.14	76.2
6	0.50	0.13	74.3
7	0.36	0.07	81.0
8	0.42	0.13	69.0
9	0.49	0.10	79.8
10	0.54	0.09	82.9
11	0.26	0.10	62.7
12	0.53	0.18	65.6
13	1.28	0.32	75.2
14	1.16	0.36	69.3
15	1.26	0.43	66.3
16	1.06	0.46	56.3

horizontal propagation or squeezing. There are some assumptions: propagation of grout is limited by the tunnel wall, $h_1 + h_2 + h_3 \leq D$ in Fig. 9; there exists propagation zone in the interface of aggregates and tunnel wall; the grouts gel simultaneously; the flow of grout is assumed to be laminar.

Referring to the phenomenon in scale model, the grout in the tunnel with poured aggregates propagates mainly in two directions, horizontal and vertical. How deep the grout can "squeeze" determines the depth of propagation of the grout, and how far the grout can penetrate during the gel time determines the horizontal penetration length of the grout.

Vertical propagation:

$$v_{zt} = v_0 - a_z t$$

$$a_z \propto \frac{K_2(1-\rho_w)}{K_1 \rho_{grout}} g$$

$$K_1 \propto e^h$$

$$K_2 = f(\text{void, gradation, } \ldots)$$

where v_{zt} is the vertical speed of grout at time t; v_0 is the initial speed of grout; a_z is vertical acceleration of grout; ρ_w is the density of water; ρ_{grout} is the density of grout; g is the gravity acceleration; K_1 is extrusion degree coefficient ($K_1 = 1$ during the Period I; $K_1 > 1$, during the Period II and III); As the grouts spread deep, the aggregate is squeezed densely, the pores become less, and the difficulty of the grouts penetration to the deeper depths will gradually increase; K_2 is a function of grout propagation in aggregates, which is related to the porosity, gradation, particle size, compactness, etc. of the aggregates ($K_1 = 1$ during the Period I); if $V_{yt} > 0$, when $h = h_1 + h_2$, the Period III begins.

According to the principle of conservation of momentum, there are:

$$m_{grout} v_0 = m_{grout} v_0' + m_w \Delta v_w + m_{aggregate} v_{aggregate}$$

$$v_{aggregate} \approx 0$$

Period I (without aggregate escaping):

$$\Delta m_{grout} \ll m_w$$

Ideally, the acceleration along the direction of the water flow is a_x, after Δt, $v_{x1} = v_w$

$$v_{x1} = v_x - a_x t = v_0 - a_x t = v_w$$

$$l_{1max} = \int_0^{\Delta t_1} v_0 + a_x t \mathrm{d}t + v_w (t_{gel} - \Delta t_1)$$

$$v_{it} = v_i + a_i \Delta t (i \in [x, y, z])$$

$$v_i = v_0 (i \in [x, y, z])$$

where m_{grout} is the mass of grout; m_w is the mass of water; $m_{aggregate}$ is the mass of aggregate; v_w is the speed of water; $v_{aggregate}$ is the speed of aggregate; v_0' is the speed of grout at time t; a_x is horizontal acceleration of grout; v_x is horizontal speed of grout; v_{x1} is horizontal speed of grout along water flow; l_{1max} is the maximum horizontal penetration length in Period I. The acceleration against the direction of the water flow is a_x, after Δt, gelling when $v_{x1} = 0$, l_2 reaching the maximum:

$$l_{2max} = v_0 t_{gel} - \int_0^{\Delta t_2} a_x t \mathrm{d}t - \int_0^{\Delta t_3} a_x t \mathrm{d}t - v_w (t_{gel} - \Delta t_1 - \Delta t_3)$$

$$a_x \propto \frac{v_w^2 \rho_w}{2 \Delta x \rho_{grout}} \text{ (can be measured)}$$

$$\text{Period II}: l_{II} = \frac{v_{yt}}{v_0} l_I$$

$$\text{Period III}: l_{III} = \frac{v_{yt}}{v_0} l_{1I}$$

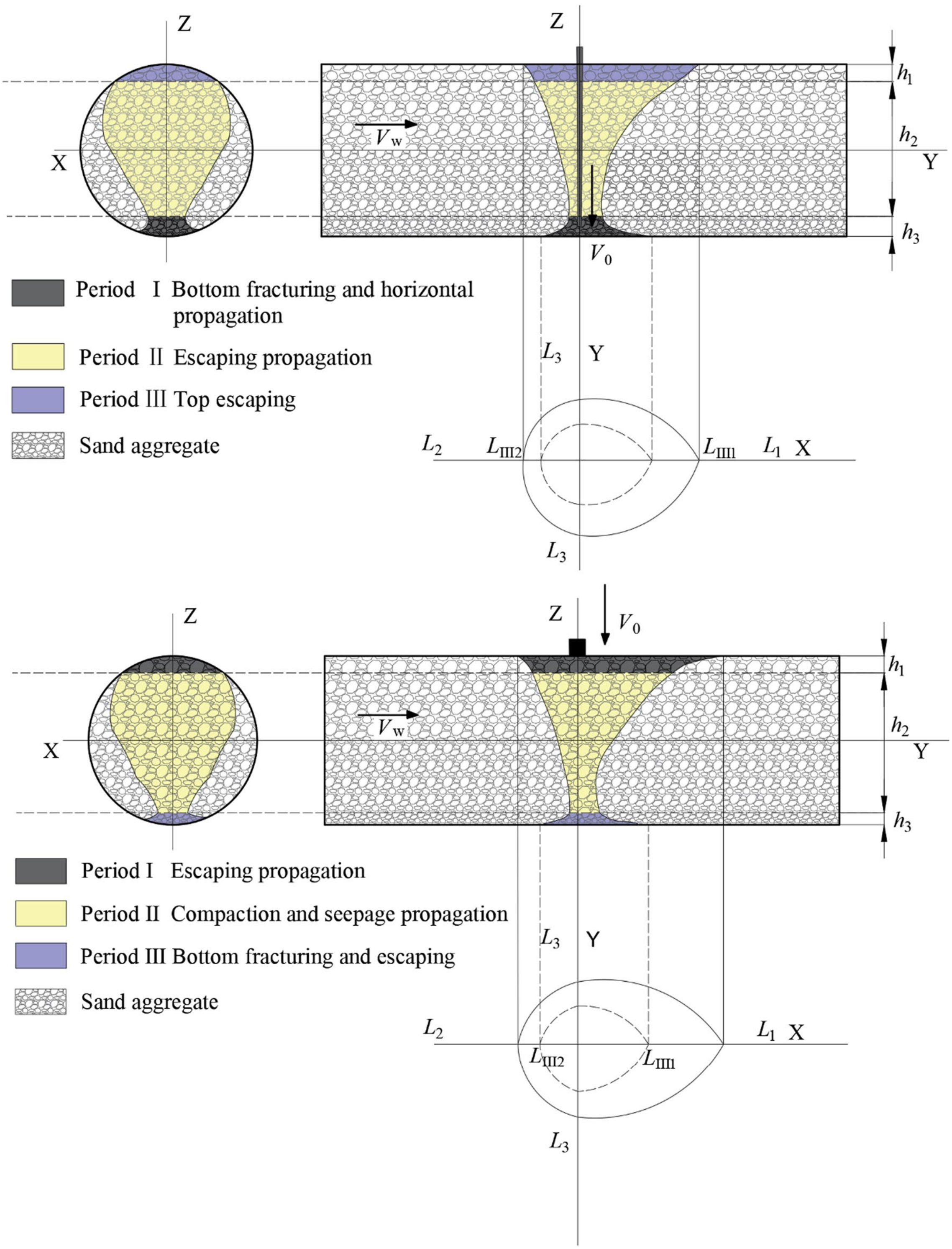

Fig. 9 Point grouting from **a.** the top of a tunnel **b.** the bottom of a tunnel

where l_2 is the maximum distance of propagation against the water flow (during condensation time); after Δt_1 the speed of grout along the direction of water flow is reduced to v_w, which is maintained until the grout solidifies; after Δt_2 the speed of grout against current is reduced to 0, while it is accelerated to v_w along the direction of water flow after Δt_3 until the grout solidifies.

Point grouting from the bottom of tunnel

When the outlet of grouting is at the bottom of the tunnel, the grout propagation can also be divided into three stages, the Period I is the bottom horizontal escaping, the Period II is the grout rising along the grouting pipe (unlike point grouting from the top, when the grout is "permeation and escaping" rather than "squeezing"), and the Period III is the grout reaches to the top and spreads horizontally at the top.

In the horizontal ascending stage, there is an uncondensed zone around the grouting pipe, and the grout flows from the non-condensed zone in the bottom dense accumulation aggregates area to the top boundary aggregate-free area.

$$a_z \propto \frac{K_2(\rho_w - 1)g}{K_1\rho_{\text{grout}}} \text{ (can be measured)}$$

$$a_x \propto \frac{v_w^2\rho_w}{2 \triangle x\rho_{\text{grout}}} \text{ (can be measured)}$$

Period I: $v_{x\text{initial}} = v_0$, outlet of grouting is at the bottom of the tunnel, therefore, the horizontal initial speed is larger than that for the case the grouting outlet at the top, resulting in a farther horizontal penetration length. Period II: as the grout fills the bottom pores, grout climbs upwards along the interface between the pipe and aggregates and the horizontal propagation is weak. Period III: currently, the horizontal initial speed of grout is smaller than that of the grouting outlet at the top, resulting a relatively shorter horizontal diffusion distance.

For the propagation of Trial no. 2, $v_w = 0.32$ cm/s, $v_0 = 1$ cm/s, $a_x \approx 0.04$ cm/s^2, $t_{\text{gel}} = 60$ s

$$t_{\text{gel}} < t - \frac{l}{v_0}$$

$$\rho_{\text{grout}} = \frac{M}{V} = \frac{m_{\text{w}} + m_{\text{cement}} + m_{\text{Sodium-Silicate-Sand}}}{v_{\text{w}} + v_{\text{cement}} + v_{\text{Sodium-Silicate-Sand}}} = 1.37 \text{ g/cm}^3$$

$$l_{\text{III}1max} = \int_0^{\Delta t_1} v_0 - a_x t\text{d}t + v_w\left(t_{\text{gel}} - \Delta t_1\right) = 154 \text{ mm}$$

$$l_{\text{III}2max} = \int_0^{\Delta t_2} v_0 - a_x t\text{d}t - \int_0^{\Delta t_3} a_x t\text{d}t - v_w\left(t_{\text{gel}} - \Delta t_1 - \Delta t_3\right) = 47 \text{ mm}$$

The measured l_{1max} is 150 mm, 97% of the calculated value; the measured $l_{\text{III}2max}$ is 50 mm, the calculated is 47 mm. Although the calculation results are basically close to the measured, it is necessary to refine the determination of the relevant coefficients in the model.

Various factors during grout propagation process in aggregates

Factors influencing grout propagation

Experiments have shown that the gel time of two-liquid grout is the primary influencing factor in the aggregate mass. During the aggregate pouring stage, the poured aggregates with different particle sizes reduce the water flow rate and transform the pipe flow into a seepage. In the grouting stage, the grout propagation is mainly in the loose accumulation area in the upper part of the aggregate mass, sealing the unconnected space at the top of the tunnel with flowing water. Therefore, the water pressure difference is not particularly significant on the success of grouting and plugging. This implies that the gel time of two-liquid grout under dynamic water conditions plays an important role in the water plugging effect in the grouting stage, and is the internal cause of the grout solidification and thus the water blocking effect.

The grouting process is different in coarse and fine aggregates. Grout filling begins in the voids among loose aggregate mass for coarse aggregates. For example, in Trails No.13, No.14, No.15, and No.16, the coarse aggregate with a particle size of 2–10 mm was used. The large void formed by the coarse-grained aggregate can provide a free flow space for grout. After the completion of filling grouting, the grout in the pressurized grouting stage enters the dense aggregate area under the action of high pressure, and the gout moves mainly in horizontal and vertical direction, and the penetration splits the aggregate mass. In the fine aggregates, the grout enters the aggregate mass within a certain radius near the grouting outlet in three modes of permeation filling, compaction, and fracturing. The loose accumulation at the top is then cemented to seal the untouched area by aggregate at the top of the tunnel. This implies that the grout mainly propagates in the top untouched area or loosely compacted coarse-grained area. This is also related to that flowing water is mainly low-speed permeation in the topped aggregate mass; while when the tunnel is not topped by aggregates, the top flow is intermittent high-speed permeation, and the middle and bottom flow is mainly low-speed permeation.

A case of pouring and grouting for blocking water inrush inundation

The Panji coal mine is in Huainan City, Anhui Province, China. The panel 12,123 has a length of 1230 m and a width of 221 m, with a cutting height of 4.14 m, an inclination angle of 5~15°. There are more than 12 normal faults and among them 3 faults with a throw of greater than 5 m. At 10:51 p.m. on May 23, 2017, the floor of the connecting tunnel in the panel inrushed with an initial flowrate of 15 m^3/h; and reached 3024 m^3/h after 48 h, much larger than the drainage capacity of the mine, resulting in the mine being flooded. The instantaneous water flow rate reached 14,000 m^3/h, with a temperature of 40~44 °C. At the same time, the water level in the Ordovician limestone aquifers in the adjacent mines dropped sharply, and the investigation and analysis showed that the water was from the Ordovician limestone karst aquifer 100 m below the bottom of the panel.

The mine adopted pouring aggregates and grouting to deal with the accident. Three directional drilling holes on the ground poured sand and gravel aggregates, the bottom was laid first and an accumulated mass was formed in the tunnel. Then, the grouting process was implemented by three stages: filling and grouting stage, increasing pressure grouting stage, reinforcement grouting stage, using aggregates with a total volume of 2114 3m^3 and cements with a mass of $15{,}515.88 \times 10^3$ kg. Finally, a water plugging section with a length of 106 m in the tunnel was formed, and the sealing efficiency reached 100%. This project was a successful case for the two stages of pouring aggregate and grouting for treatment of inundation of an underground tunnel.

Limitations and further study

In this paper, the primary and secondary order of the factors affecting the effect of sealing efficiency in different grades of aggregates in the inundated tunnel was obtained, and the water pressure changes, water flow rate, grouts propagation mode and shape of grouted mass were investigated and analyzed. These understandings make up for the shortcomings of previous research; however, there are still some problems that deserve further in-depth study.

For example, in the two stages of pouring aggregate and grouting, there are more factors affecting the sealing efficiency than investigated in this work. Other factors, such as grouting pressure, roughness, inclination of tunnel surface, grout take should be subsequently considered in future works. For another example, the actual section of tunnel is often not circular, and the transport and solidification of the grouts in the tunnel with different cross-section shapes, and the effect of grout sealing after aggregates pouring under variable or mixed particle sizes should be further studied. In the on-site grouting and plugging project, the bottom of tunnel is usually laying with fine grains and the upper area is then filled with coarse aggregates. After the pipeline flow becomes seepage, grouting is supplemented to seal the aggregate void to block water. Subsequent studies will make them closely relevant to the actual project. In addition, variation of permeability during grouting process should be further investigated also.

Conclusion

This work focused on the second stage in the control of an inundated underground tunnel due to water inrush, i.e., the grouting stage, after the first stage aggregates pouring stage, to investigate the main effects on sealing efficiency, water pressure variation during grouting, propagation mechanism of grouting in the poured aggregates with different grain sizes and flowing water. The main conclusions are as follows:

Results of an orthogonal array with four factors and four levels indicated that the main effects on the sealing efficiency of grouting in poured aggregates with flowing water in a descending order is cement slurry/sodium silicate ratio, relative density of aggregates, particle size of aggregates, and final water pressure difference between both ends of aggregates segment.

The variation of pore water pressure during grouting in the poured aggregates with different particle sizes showed that the curves of water pressure at different measured points have the same trend, which reflects the consistency of water flowing and grout propagation in the tunnel. The variation type of water pressure presented four categories; overall ascending, step ascending, concave, and convex type, which mainly depends on water pressure, water flowrate, relative density and grain size of aggregates, gel time, propagation mechanism of grout.

The final cementation form of grouted aggregates found through layer-by-layer excavation can be divided into four shapes: T, H, O and shell shape. The main grout propagation mode includes three types: permeation filling, compaction-permeation, and compaction-fracturing mode, which reflects the influence of grain size, density of aggregates and grouting pressure.

The flow rate after grouting has decreased by approximately 60% to 86% compared to that before grouting, bulk hydraulic conductivity decreased by more than 80%, reflecting a great improvement of the sealing efficiency in the grouting stage after the aggregate pouring stage.

Acknowledgements
The authors thank the National Natural Science Foundation of China for the provided support under Grant nos. 42130706 and 41877238.

Author contributions
WS and GZ proposed the main idea of this study and designed the experiments. ZL, RL and DM performed the experiments and analyzed the results, JL deduced the theoretical expression of propagation. ZL, GZ and WS prepared the manuscript. All authors have read and approved the final manuscript.

Funding
This study was supported by the National Natural Science Foundation of China under Grant nos. 42130706 and 41877238.

Availability of data and materials
All data generated or analyzed in this study are included in the published article.

Declarations

Competing interests
The authors declare that they have no competing interests.

Author details
[1]School of Resources and Geosciences, Institute of Mine Water Hazard Prevention and Control Technology, China University of Mining and Technology, Xuzhou 221116, China. [2]Chongqing Architectural Design Institute Co., LTD, Chongqing 400010, China. [3]National Coal Mine Water Hazard Prevention Engineering Technology Research Center, Suzhou 234000, Anhui, China. [4]Shanghai Urban Construction Design and Research Institute (Group) Co., Ltd, Shanghai 200125, China.

Received: 29 December 2022 Accepted: 31 May 2023
Published online: 10 June 2023

References
Chang H (2004) Hydraulic fracturing in particulate materials. Georgia Institute of Technology
Dong SN, Yang ZB, Zhu MC, Zhang WZ, Shi L, Mu L (2020) Development of large-scale simulation experiment system of dynamic water rapid sealing in flowing water roadway. J China Coal Soc 45(09):3226–3235
Gao Y, Sui WH (2016) Modelling of chemical grout column permeated by water in transparent soil. Int J Environ Pollut 59(2–4):142–155
Hu W (2016) Experimental investigation on the mechanism of grouting and plugging of water inrush in underground engineering rock mass. Wuhan University Press, Wuhan
Hui S, Sui WH, Zhang GL, Chen JX, Yu SB (2022) Plugging efficiency of pouring aggregates through multiple boreholes into an inundated tunnel to prevent groundwater inrush disasters. Geoenviron Disasters 9:15. https://doi.org/10.1186/s40677-022-00217-2
Jiang XM, Hui S, Sui WH, Shi ZY, Wang JH (2020) Influence of the aggregate-pouring sequence on the efficiency of plugging inundated tunnels through drilling ground boreholes. Water 12:2698
Karol RH (2003) Chemical grouting and soil stabilization, revised and expanded. CRC Press, Boca Raton
Krizek RJ, Perez T (1985) Chemical grouting in soils permeated by water. J Geotech Eng 111(7):898–915
Li SC, Liu RT, Zhang QS, Zhang X (2016) Protection against water or mud inrush in tunnels by grouting: a review. J Rock Mech Geotech Eng 8(5):753–766
Li S, Zhang J et al (2019) Investigation and practical application of a new cementitious anti-washout grouting material. Constr Build Mater 224:66–77
Liang Y, Sui W, Qi JF (2019) Experimental investigation on chemical grouting of inclined fracture to control sand and water flow. Tunn Undergr Space Technol 83:82–90
Liu Q, Chen WZ, Yuan JQ, Zhang QY, Rong C, Wang SQ, Zhao LT (2019) Laboratory experiment study of grouted materials filled in karst caverns. Chin J Rock Mech Eng 38(S1):3179–3188
Mohammed MH, Pusch R, Knutsson S (2015) Study of cement-grout penetration into fractures under static and oscillatory conditions. Tunn Undergr Space Technol 45:10–19
Mu L, Dong SN (2020) Migration rule and water blocking mechanism of cement slurry in aggregate accumulation of underground tunnel closure. Chin J Undergr Space Eng 16(06):1891–1900
Ni MG (2014) Experimental investigation of grouting into rich water sand stratum. Beijing: China University of Geosciences (Beijing)
Nichols SC, Goodings DJ (2000) Effects of grout composition, depth and injection rate on compaction grouting. In: GEO-DENVER 2000 Advances in grouting and ground modification, Denver, Aug.5–8, pp 16–31. https://doi.org/10.1061/40516(292)2.
Ren KC (1982) Flow law and grouting method of chemical grouting with flowing water. Water Conserv Hydropower Technol (7):59–63+52
Sui WH, Liu JY, Hu W, Qi JF, Zhan KY (2015) Experimental investigation on sealing efficiency of chemical grouting in rock fracture with flowing water. Tunn Undergr Space Technol 50(1):239–249
Wang DL (2011) Mechanism of hydro-dynamically chemical grouting in porous media. Ph. D. thesis, China University of Mining and Technology, Xuzhou, China
Zhan KY, Sui WH, and Gao Y (2011) A model for grouting into single fracture with flowing water. Rock Soil Mech 32(6):1659–1663, 1689
Zhang GL (2016) An experimental investigation on the permeability of chemically grouted sands and its application for mitigating underground sand and water inrushes. Int J Environ Pollut 59(2–4):187–202
Zhang GL, Zhan KY, Gao Y, Wang WX (2011) Comparative experimental investigation of chemical grouting into a fracture with flowing and static water. Min Sci Technol (china) 21(2):201–205
Zhang LZ, Zhang QS, Zhang X, Li ZP, Wang DM, Zhao P (2017) On the diffusion mechanism of permeation grouting under hydrodynamic conditions. Mod Tunnel Technol 54(01):74–82
Zhang GL, Hui S, Li WX, Sui WH (2020) Experimental investigation on pouring aggregate to plug horizontal tunnel with flow water. Water 12:1763

Publisher's Note